


Article

Experimental Study on the Aerodynamic Performance and Wave Energy Capture Efficiency of Square and Curved OWC Wave Energy Conversion Devices

Xueyan Li ^{*}, Zhen Yu, Hengliang Qu ^{*}, Moyao Yang, Hongyuan Shi  and Zhenhua Zhang

Coast Institute & Institute of Sea-Crossing Engineering, Ludong University, Yantai 264025, China

^{*} Correspondence: yanzi03@126.com (X.L.); quhengliang@ldu.edu.cn (H.Q.)

Abstract: To develop novel wave energy conversion devices (WECDs) with excellent performance, the relative wave height and pressure in the chambers of square and curved oscillating water column (OWC) WECDs were compared through physical model tests, and the effects of regular incident wave factors, the opening length, the opening width, and the chamber volume on the aerodynamic performance and wave energy capture efficiency (WECE) of the WECDs were investigated. The results indicated good chamber performance for both the square and curved OWC WECDs. As the incident wave height increased, the wave surface elevation, WECE, and pressure in the chamber all increased, while the relative wave height in the chamber decreased. When the opening length, width, and area of the WECD increased, both the relative wave height and chamber pressure increased. The relative wave height in the chamber increased with decreasing chamber volume; however, the chamber pressure and intrachamber WECE decreased with increasing chamber volume. It is recommended that, in actual engineering applications, the overall efficiency of the device be improved by increasing the opening length, width, area and volume of the air chamber.

Keywords: wave energy conversion devices; physical model tests; chamber operating performance; wave energy capture efficiency



Citation: Li, X.; Yu, Z.; Qu, H.; Yang, M.; Shi, H.; Zhang, Z. Experimental Study on the Aerodynamic Performance and Wave Energy Capture Efficiency of Square and Curved OWC Wave Energy Conversion Devices. *Sustainability* **2023**, *15*, 4963. <https://doi.org/10.3390/su15064963>

Academic Editor: Adem Akpınar

Received: 16 February 2023

Revised: 8 March 2023

Accepted: 8 March 2023

Published: 10 March 2023



Copyright: © 2023 by the authors. Licensee MDPI, Basel, Switzerland. This article is an open access article distributed under the terms and conditions of the Creative Commons Attribution (CC BY) license (<https://creativecommons.org/licenses/by/4.0/>).

1. Introduction

New clean and renewable energy systems must be built to reach peak carbon dioxide emission and carbon neutrality targets against an increasingly challenging background of energy supply and demand, climate change, and energy insecurity. The ocean represents abundant pollution-free energy. For example, wave energy has broad development prospects due to its large reserve [1–3] and high flow density [4–6]. Traditional oscillating water column (OWC) wave energy conversion devices (WECDs) [7,8] have a high cost and a low wave energy conversion efficiency; moreover, focused wave groups can excite harbor resonance [9,10]. The incident wave direction significantly affects the highest rise and strength of the harbor resonance. However, traditional WECDs cannot satisfy the requirements of modern ports due to their limited application range in the sea area. In addition, traditional WECDs cannot fully exploit wave energy due to the single structural model used for their study.

Researchers have conducted in-depth studies on the use of structural advantages to develop new high-efficiency WECDs [11–14]. Ning et al. [15,16] investigated the effects of the chamber width, gas orifice size, and bottom slope of an OWC device on its wave energy conversion efficiency and found that the wave energy capture efficiency (WECE) of a dual-chamber device was superior to that of a single-chamber device through experimental and numerical analyses. Zhao [17] found experimentally a higher wave energy conversion efficiency for a dual-chamber OWC device than a single-chamber OWC device. With the continuous in-depth study of WECDs, Simeon et al. [18] proposed the design idea of an M-OWC, summarized the development status of WECDs, and provided some new insights for

the use of OWC devices. Du et al. [19,20] calculated the chamber pressures of OWC devices under multiple operating conditions (square or cylindrical chamber bottoms, asymmetrical front and back walls, etc.) with the three-dimensional Green function to investigate the influences of the incident wave factors on the wave energy conversion efficiency of the OWC devices.

Based on the design concept of a permeable breakwater, Zhou [21] divided an OWC WECD into two parts, comb teeth and chambers, and found that a comb tooth with a specific length had multiple effects, including wave suppression and energy gathering. The permeable breakwater has a low construction cost and can effectively reduce wave reflection and the wave force and effectively absorb wave energy. An excellent wave energy conversion effect can be achieved by combining the permeable breakwater with a WECD. Therefore, WECDs with new structures that facilitate the free exchange of water and significantly reduce construction costs, namely, square and curved OWC WECDs, are proposed in this paper. The effects of factors such as incident wave factors, the chamber opening size, and the chamber volume on the aerodynamic performance and WECE of the chambers of square and curved WECDs were investigated through physical model tests.

2. Physical Model Test Design

2.1. Model Design

As shown in Figures 1 and 2, each device was composed of comb teeth, wing plates, a front wall opening, an energy capture chamber, a front wall, and permeable troughs. The width and length of each comb tooth were 0.15 m and 0.3 m, respectively. The width and length of the energy capture chamber were both 0.3 m. The width and height of the front wall were both 0.3 m. The wing width and height were 0.8 m and 0.7 m, respectively. The width and height of each permeable trough were 0.1 m and 0.4 m, respectively. The height of the structure was 0.7 m. The size of the top opening was $0.04 \text{ m} \times 0.04 \text{ m}$, and the size of the underwater front wall opening was designed according to each working condition. Holes were made on trough plates of the same size, and different opening rates of the energy capture chamber were achieved by replacing the trough plates.

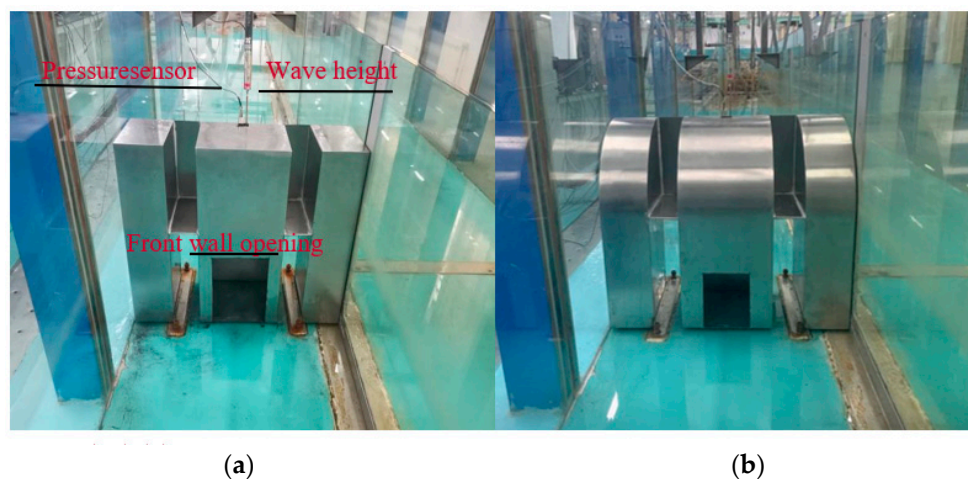


Figure 1. Structural models of (a) squared and (b) curved WECDs for the physical tests.

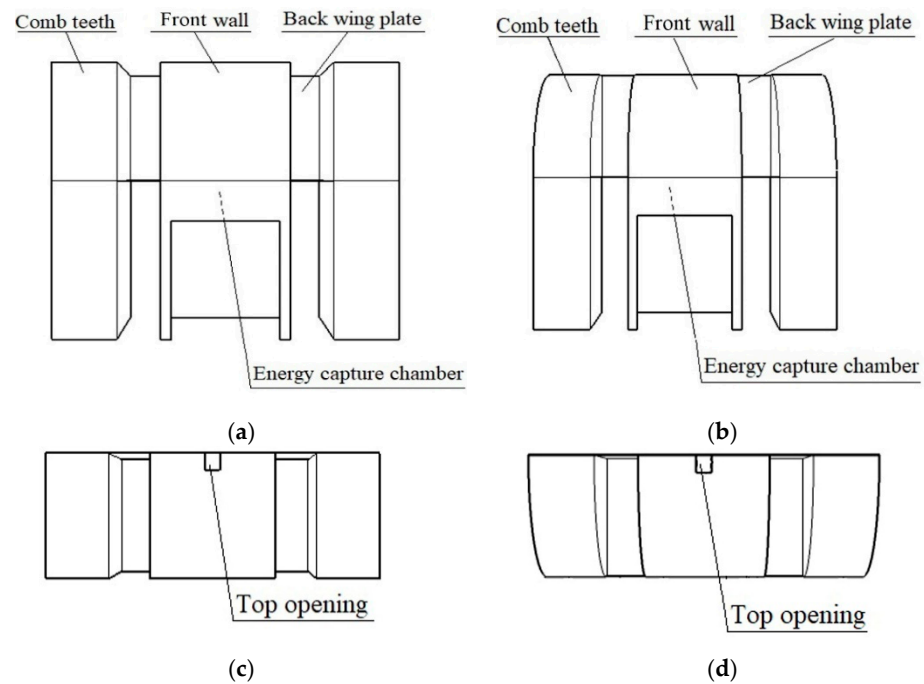


Figure 2. Schematic structural diagrams of the square and curved WECDs. Front views of the (a) square and (b) curved WECDs and top views of the (c) square and (d) curved WECDs.

2.2. Test Setup

Experiments were conducted in a wave–current flume of the Port, Waterway and Coastal Engineering Experimental Center of Ludong University. The flume was 60 m long, 0.8 m wide, and 1.8 m high, and the test water depth was 0.4 m. The structural model was placed at 30 m from the wave-making area of the test flume, and a wave height meter was installed at the fixed structure. The wave height test data from the wave height meter were detected and calibrated to meet the design requirements for wave height. Gravel (average gravel particle size: 100–150 mm) was placed at the end of the tank to eliminate wall-end reflection. The slope of the gravel beach was 1:5, with a length of 6.8 m and height of 1.3 m. In the experiment, the wave height meter and pressure sensor were used for data measurement, and the structure was placed in the test flume to complete the test simulation. The wave height meter and pressure sensor were both placed at the top opening of the square or curved WECD, and the wave height and pressure in the chamber were measured by a DS-30 data acquisition instrument.

2.3. Test Conditions

The physical test parameters are shown in Table 1. The square and curved WECDs were experimentally compared under the same conditions of water depth and incident waves with different heights and periods. According to the preliminary study, the regular wave conditions were as follows: water depth $d = 0.4$ m, wave height $H = 0.04$ m and 0.08 m, and period $T = 1.0$ s, 1.2 s, 1.4 s, 1.6 s, 1.8 s, and 2.0 s.

Table 1. Test parameters.

Parameter	Unit	Values
Water depth d	m	0.4
Wave height H	m	0.04, 0.08
Period T	s	1.0, 1.2, 1.4, 1.6, 1.8, 2.0
Wavelength L	m	1.46, 1.94, 2.39, 2.84, 3.27, 3.69

Table 2 shows the model parameters. The chamber volume of the square or curved WECD was changed by adjusting the proportion of filling in the chamber. As the amount of filling increased, the chamber volume decreased. The ratio of V1, V2 and V3 was 4:3:2.

Table 2. Model parameters.

Type	Number	Opening Width (m)	Opening Length (m)	Opening Area (m ²)	Chamber Volume (m ³)
Square/curved	W15H20	0.15	0.20	0.030	0.027/0.021
	W15H25	0.15	0.25	0.038	0.027/0.021
	W15H30	0.15	0.30	0.045	0.027/0.021
	W20H30	0.20	0.30	0.060	0.027/0.021
	V1	0.20	0.30	0.070	0.027/0.021
	V2	0.25	0.30	0.070	0.020/0.016
	V3	0.25	0.30	0.070	0.014/0.011

3. Results and Discussion

For the purpose of exploring the aerodynamic performance and wave energy capture efficiency (WECE) of square and curved OWC WECDs, this paper compares the results with those of Ning et al. [22], as shown in Figure 3. The results indicate that both the aerodynamic performance and WECE of square and curved OWC WECDs are satisfactory within the scope of the test, thus providing a theoretical basis for future engineering construction.

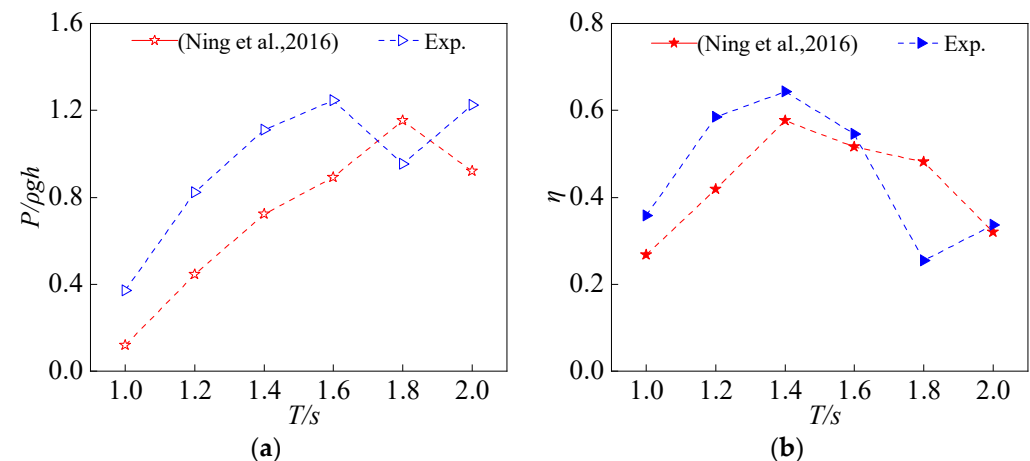


Figure 3. Comparison of test results with those of Ning et al. (2016) [22]: (a) period -dependent curves of the chamber pressure; and (b) period-dependent curves of the WECE.

3.1. Comparison and Analysis of the Aerodynamic Performance

Within the scope of the experiment, the compressibility of the air in the chamber was negligible. Therefore, the airflow in the chamber was regarded as an incompressible flow. The required test pressure was calculated using the flow field velocity function [23]. The effects of the incident wave factors, the size of the chamber opening, and the volume of the energy capture chamber on the aerodynamic performance of the square and curved WECDs were comparatively analyzed to identify the best WECD structure.

3.1.1. Effects of the Incident Wave Factors

Two model structures of the same size were selected. The opening of the energy capture chamber was 0.15 m wide and 0.25 m long. The ratio of the wave height H' to the incident wave height H in the chamber (H'/H) was defined as the relative wave height. Figure 4 compares the period-dependent curves of the relative wave height and the chamber pressure of the square and curved WECDs under incident waves with different heights ($H = 0.04$ m and 0.08 m) and periods ($T = 1.0$ s, 1.2 s, 1.4 s, 1.6 s, 1.8 s, and 2.0 s).

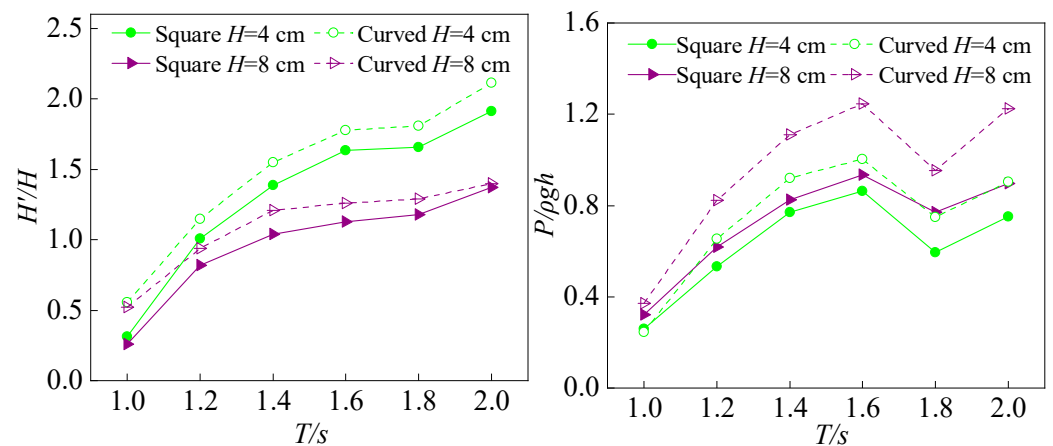


Figure 4. Period-dependent curves for different incident wave heights of the relative wave height and chamber pressure, for the square and curved WECDs, respectively.

The figure indicates that a larger incident wave height results in a lower relative wave height in the chambers of the square and curved WECDs. For small to medium periods ($T = 1.0\text{--}1.6$ s), the relative wave heights in the chambers increased with the incidence period. For long periods ($T = 1.6\text{--}2.0$ s), the chamber pressures of different WECDs increased with the incident wave height, indicating that a higher incident wave height resulted in a higher fluctuation amplitude of the water surface in the chamber and a higher chamber pressure. As the period of the incident wave increased, the chamber pressures of the square and curved WECDs first increased, then decreased, and then increased again, indicating a relatively large chamber pressure for a specific incident period. The relative wave height and chamber pressure of the curved WECD were always higher than those of the square WECD.

3.1.2. Effect of the Opening Length

The chamber opening of the square or curved WECD was set using a fixed width of 0.15 m and different lengths (0.20 m, 0.25 m, and 0.30 m). The three models corresponding to the three chamber opening dimensions were defined as W15H20, W15H25, and W15H30. The tests were performed under incident waves with different periods and a fixed height ($H = 0.04$ m). Figure 5a compares the relative wave heights in the chambers of the square and curved WECDs, and Figure 5b compares the chamber pressures of the square and curved WECDs.

The figure indicates that for a fixed period of the incident wave, the opening length had a significant impact on the relative wave heights in the chambers of the square and curved WECDs and that when the other factors were fixed, the relative wave height and pressure increased with the opening length. At a fixed opening length and increasing incidence wave period, the relative wave heights in the chambers of the square and curved WECDs increased and the chamber pressure first increased, then decreased and then increased again. Increasing the opening length enhanced the aerodynamic performance of the chambers of the square WECDs, and even more, that of the curved WECD.

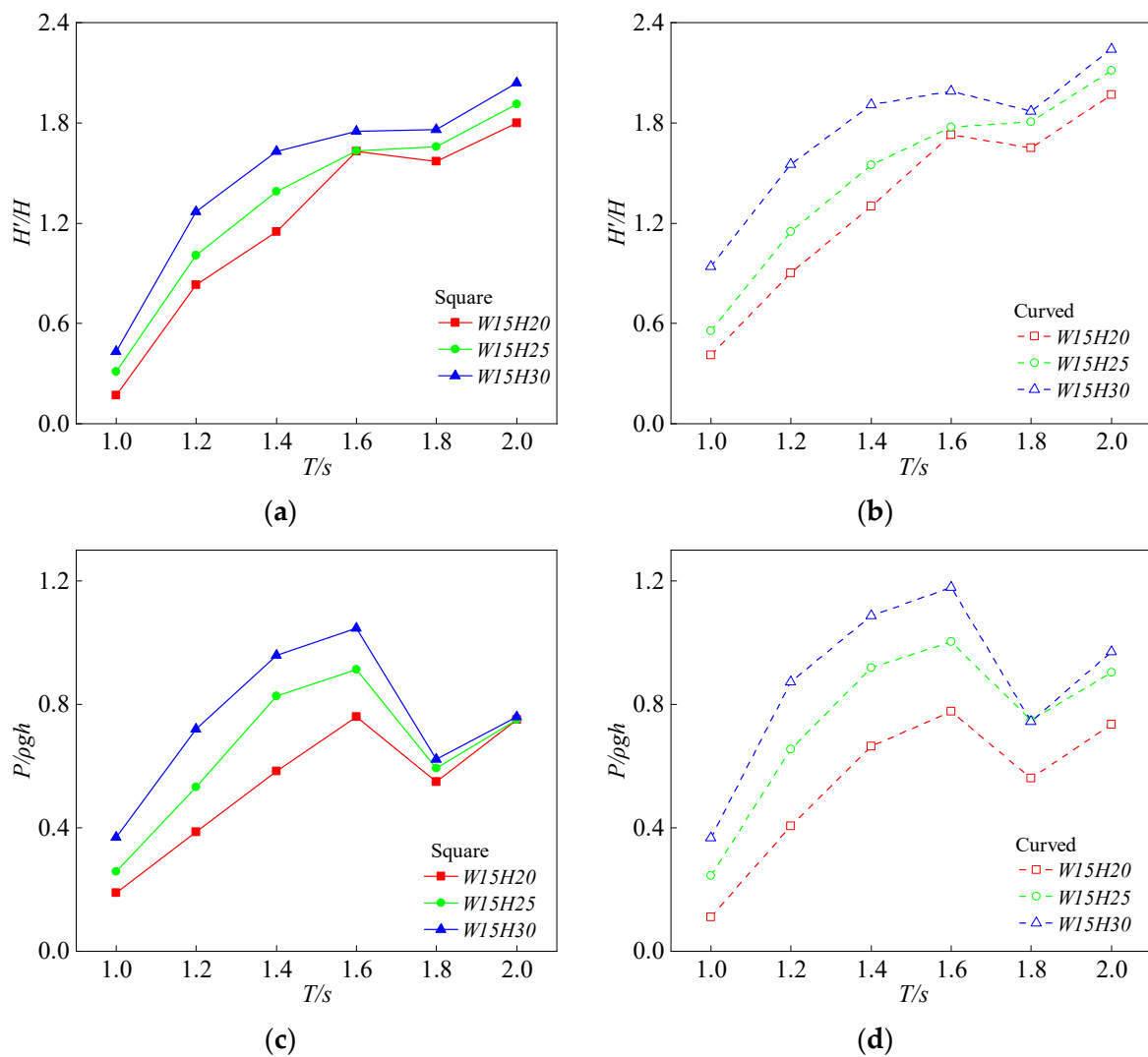


Figure 5. Effects of the opening length on the chamber performance of the square and curved WECDs. Period-dependent curves for different opening lengths of (a,b) the relative wave height and (c,d) the chamber pressure, for the square and curved WECDs, respectively.

3.1.3. Effect of the Opening Width

When the water depth d was 0.4 m, the chamber opening of the square or curved WECD was set at a fixed height of 0.3 m and at different widths (0.15 m, 0.20 m, and 0.25 m). The three models corresponding to the three chamber opening dimensions were defined as $W15H30$, $W20H30$, and $W25H30$. The tests were performed under incident waves with different periods and a fixed height ($H = 0.04$ m). Figure 6a compares the relative wave heights of the square and curved WECDs, and Figure 6b compares the chamber pressure of the square and curved WECDs.

The figure reveals that at the same period of the incident wave, the relative wave height in the chambers of the square and curved WECD increased as the opening width increased; however, the effect of the opening width was smaller than that of the opening length. As the opening width increased, the chamber pressure in the square and curved WECDs increased. At the same opening width, the relative wave height in the chamber of the square WECD continuously increased as the period of the incident wave increased, while the relative wave height in the curved WECD first increased, then decreased, and then increased again. The chamber pressures in the square and curved WECDs both increased initially, then decreased, and then increased again.

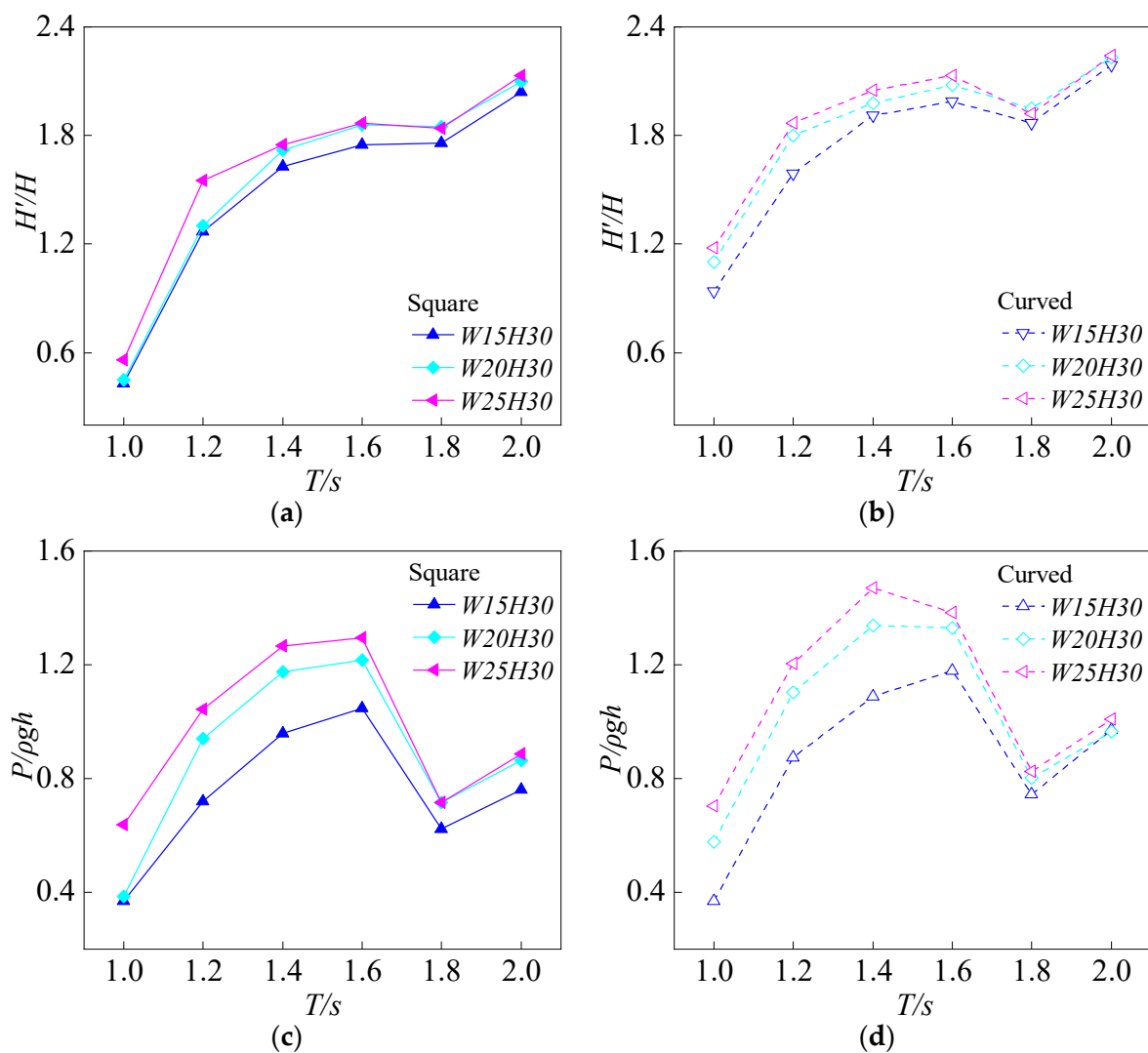


Figure 6. Effects of the opening width on the chamber performance of the square and curved WECDs. Period-dependent curves for different opening widths of (a,b) the relative wave height and (c,d) the chamber pressure, for the square and curved WECDs, respectively.

3.1.4. Effect of the Opening Area

When the water depth d was 0.4 m, the models W15H20, W15H35, W15H30, W20H30, and W25H30 were used to compare the effects of different opening areas on the square WECDs to those on the curved one (0.030 m², 0.038 m², 0.045 m², 0.060 m², and 0.075 m²). The tests were performed under incident waves with different periods and a fixed height ($H = 0.04$ m). Figure 7a compares the period-dependent curves of the relative wave heights for the square and curved WECDs, and Figure 7b compares the period-dependent curves of the chamber pressures for the square and curved WECDs.

The figure indicates that as the incidence wave period increased, the relative wave height in the chamber of the square WECD also increased, but peaked in that of the curved WECD. The relative wave heights in the chambers of the square and curved WECDs increased as the opening area increased because the increase in the opening area increased the volume of water entering the chamber, causing the wave surface to rise. The chamber pressure also increased as the opening area increased, indicating that more wave water entered the chamber. The chamber pressure first increased, then decreased, and then increased again as the period of the incidence wave increased.

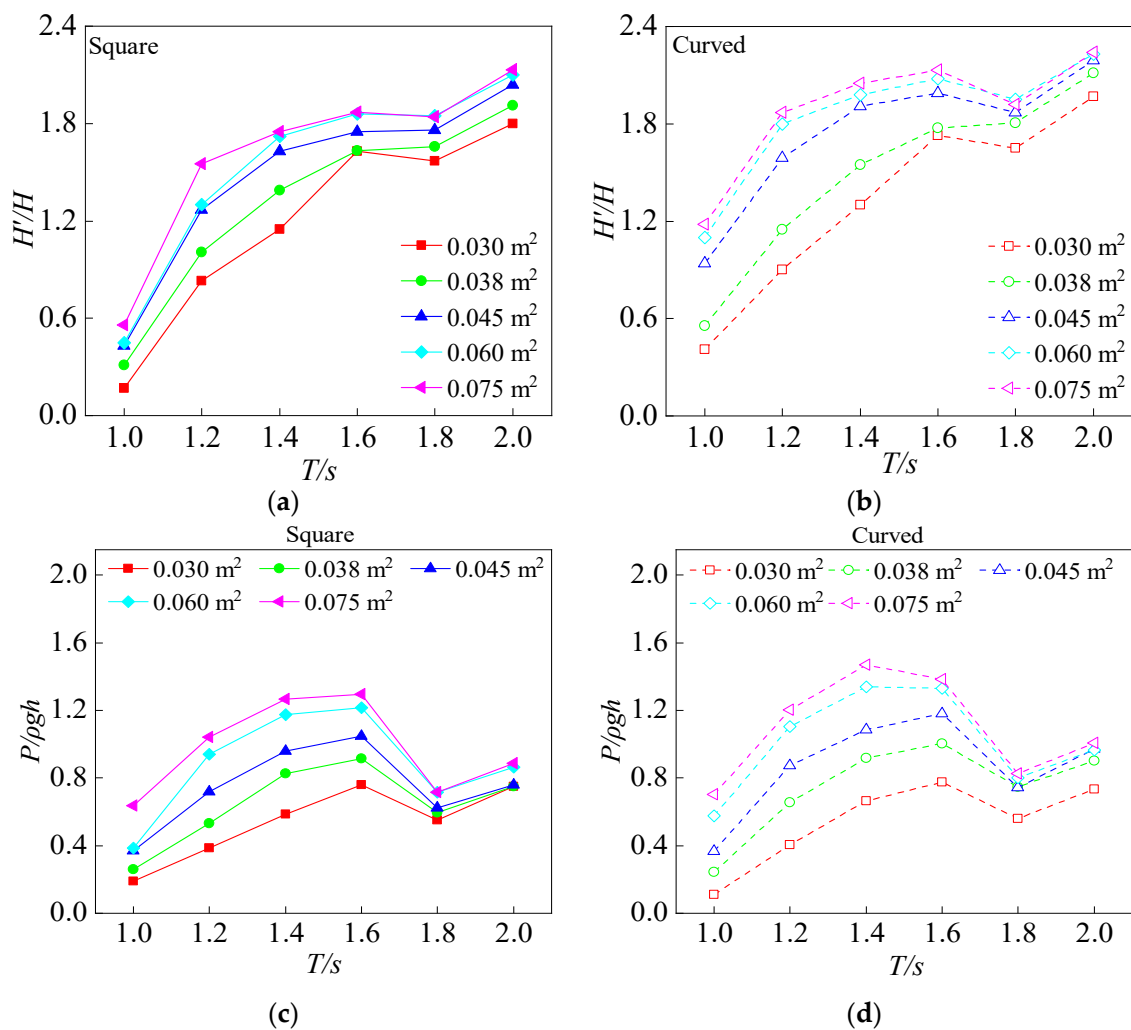


Figure 7. Effects of the opening area on the chamber performance of the square and curved WECDs. Period-dependent curves for different opening areas of (a,b) the relative wave height and (c,d) the chamber pressure, for the square and curved WECDs, respectively.

3.1.5. Effect of the Chamber Volume

At a water depth d of 0.4 m, the chamber opening of the square and curved WECDs was 0.3 m long and 0.25 m wide. Different volumes defined as V_1 , V_2 , and V_3 were used to compare the effects of chamber volume on the square WECDs to those on the curved one. The ratio of V_1 , V_2 , and V_3 was 4:3:2. The tests were performed under incident waves with different periods and a fixed height ($H = 0.04$ m). Figure 8a compares the period-dependent curves of the relative wave height for the square and curved WECDs, and Figure 8b compares the period-dependent curves of the chamber pressures for the square and curved WECDs.

Within the range of the incident wave periods in this experiment, as the chamber volume decreased, the change in the relative wave height in the chamber increased. When the chamber volume decreased by 1/4 (V_2), the trend of the relative wave height in the chamber was the same as that before the change in the chamber volume; that is, the relative wave height first increased, then started to decrease at $T = 1.6$ s, and then increased again at $T = 1.6$ s. When the chamber volume decreased by 1/2 (V_3), the trend of the relative wave height in the chamber was different from that at other chamber volumes (the relative wave height first increased, then started to decrease at $T = 1.2$ s, and then increased again at $T = 1.8$ s), and the chamber pressure decreased as the chamber volume increased. Although the square and curved WECDs showed the same pattern of variation

in the chamber pressure with the chamber volume, their chamber pressures were different. The chamber volume had a significantly different effect on the aerodynamic performance of the chamber compared with the other factors. When the chamber volume decreased, the chamber pressure of the curved WECD was lower than that of the square WECD because the air volume in the curved WECD chamber was smaller than that in the square WECD due to the smaller volume of the curved WECD.

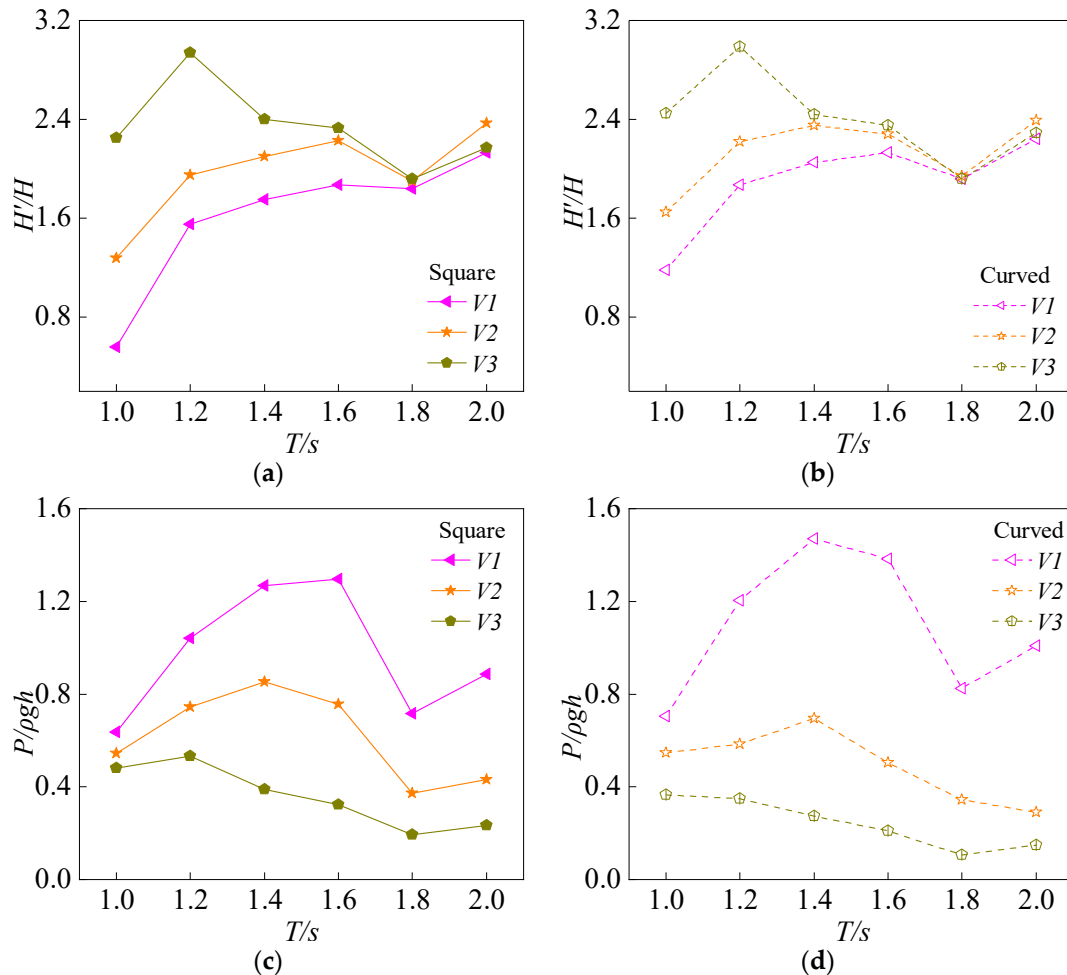


Figure 8. Effects of the chamber volume on the chamber performance of the square and curved WECDs. Period-dependent curves for the different chamber volumes of (a,b) the relative wave height and (c,d) the chamber pressure, for the square and curved WECDs, respectively.

3.2. Comparative Analysis of the WECE

The WECE (η) is an important indicator for evaluating the power generation capacities of square and curved WECDs. The WECE of each WECD was calculated according to the air pressure in the chamber of the WECD [24]:

$$P_i = \frac{B}{T} \int_{t_0}^{t_0+T} \sqrt{\frac{2|p(t)|^3}{\rho_a C_f}} dt \tag{1}$$

$$C_f = \left(\frac{1}{\alpha C_c} - 1 \right)^2 \tag{2}$$

$$\begin{cases} C_c = \tanh\left(\frac{\pi\delta}{2D_h}\right) - 0.4\tanh\left(\frac{5\pi\delta}{T^*D_h}\right), 0.5 < \delta/D_h \leq 2.01, T^* = \frac{T}{\sqrt{\delta/g}} \\ C_c = 0.61, \delta/D_h < 0.5 \end{cases} \tag{3}$$

where P_i is the average wave energy conversion power of the chamber, B is the width of the chamber, T is the period of the incident wave, $P(t)$ is the pressure in the chamber at time t , ρ_a is the air density (at 20 °C, 1.205 kg/m³), C_f is the quadratic loss coefficient, C_c is the shrinkage coefficient, δ is the wall thickness of the model template, and D_h is the diameter of the air inlet.

The WECE can be expressed as follows:

$$\eta = P_i / P_{inc} \quad (4)$$

3.2.1. Effects of the Incident Wave Factors

Figure 9 shows the period-dependent curves of the effects of the incident wave factors on the WECE of the WECDs. The specific parameters are described in Section 3.1.1. As the incident wave height increased, the WECE of the WECDs significantly decreased. When the period of the incident wave T was 1.4 s, the WECE of both the square and curved WECDs was the largest. When H was 0.04 m, the WECE values of the square and curved WECDs reached 30.8% and 35.3%, respectively, and when H was 0.08 m, they reached 22.8% and 30.1%, respectively. The incident wave height and the WECE of the curved WECD were higher than those of the square WECD. Comparative analysis of the period-dependent curves of the wave energy conversion efficiency of the square and curved WECDs revealed that both WECDs had the same WECE trend but greatly different WECE values. This result indicates that the structural form of a WECD has a significant impact on its WECE.

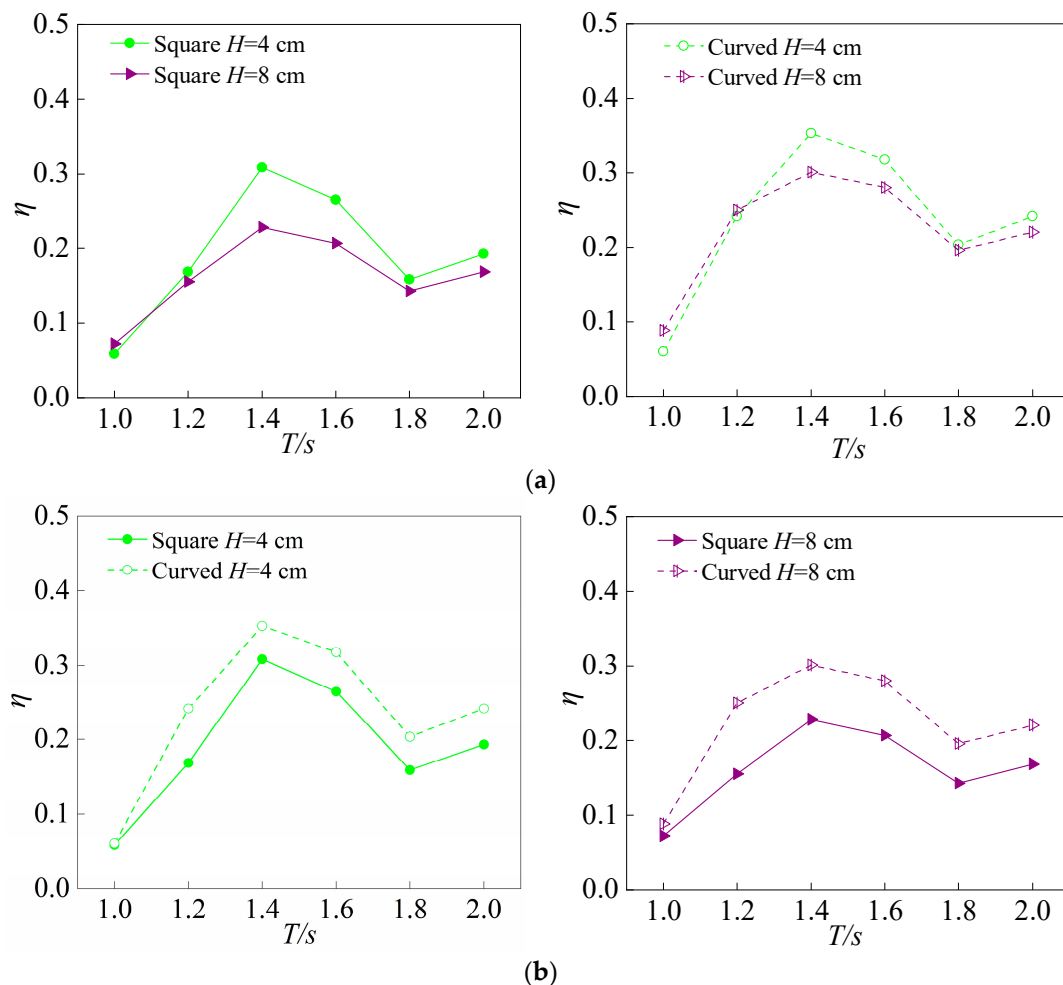


Figure 9. Effects of the incident wave factors on the WECE values of the square and curved WECDs. Period-dependent curves of the WECE of the square and curved WECDs (a) at different incident wave heights and (b) at the same incident wave heights.

3.2.2. Effect of the Opening Length

Figure 10a compares the period-dependent curves of the WECE of the square and curved WECDs for different opening lengths. Figure 10b compares the period-dependent curves of the WECE between the square and curved WECDs for the same opening lengths. The specific parameters are described in Section 3.1.2.

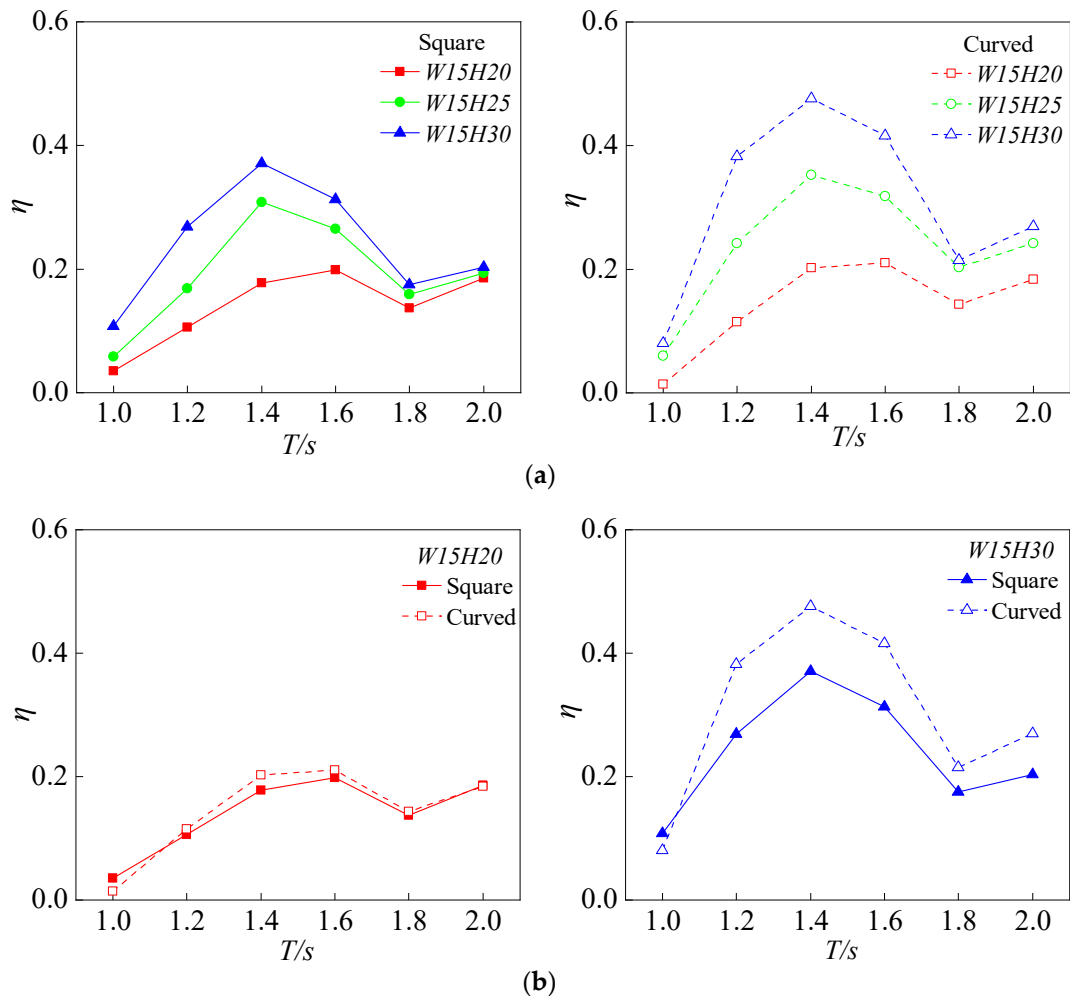


Figure 10. Effects of the opening length on the WECE values of the square and curved WECDs. Period-dependent curves of the WECE of the square and curved WECDs (a) at different opening lengths and (b) at the same opening lengths.

The figure demonstrates that the WECE increased with the opening length. At different opening lengths, the WECE peaked at different periods of the incident wave, mainly in the range of $T = 1.2$ s to 1.6 s, indicating that the largest WECE occurred within a specific range of incident wave periods. At an opening length of 0.2 m, the highest intrachamber WECE values of the square and curved WECDs were 16.0% and 17.6%, respectively; at an opening length of 0.25 m, the highest WECE values were 24.7% and 30.4%, respectively; and at an opening length of 0.3 m, the highest WECE values were 31.7% and 42.5%, respectively. At opening lengths of 0.2 m, 0.25 m, and 0.3 m, the difference in the intrachamber WECE between the square and curved WECDs was 1.6%, 5.7%, and 10.8%, respectively, indicating that the difference between the WECE values of the square and curved WECDs increased with the opening length. In particular, as the opening length increased, the intrachamber WECE of the curved WECD surpassed that of the square WECD.

3.2.3. Effect of the Opening Width

Refer to the experimental models and test conditions of 3.1.3. With regards the opening width, Figure 11 shows the period-dependent curves of its effect on the WECE values of the square and curved WECDs. The specific parameters are described in Section 3.1.3. The figure indicates that as the opening width increased, the intrachamber WECE increased. The effect of the opening width on the intrachamber WECE was smaller at large periods ($T = 1.8$ s and 2.0 s) than at small to medium periods ($T = 1.0$ s, 1.2 s, 1.4 s, and 1.6 s), and the highest intrachamber WECE values occurred at medium periods, indicating that the period of the incident wave corresponding to the optimal WECE peak was not affected by the opening width. When the opening width was 0.15 m, the intrachamber WECE values of the square and curved WECDs were 31.3% and 42.7%, respectively. When the opening width was 0.2 m, the intrachamber WECE values of the square and curved WECDs were 39.6% and 58.9%, respectively. When the opening width was 0.25 m, the WECE values of the square and curved WECDs reached 50.9% and 61.9%, respectively. At opening widths of 0.15 m, 0.20 m, and 0.25 m, the difference in the intrachamber WECE between the square and curved WECDs was 11.4%, 19.3%, and 11.9%, respectively. The intrachamber WECE values of the curved WECD at different opening widths were always greater than those of the square WECD. As the opening width increased, the difference between the intrachamber WECE values of the square and curved WECDs first increased and then decreased.

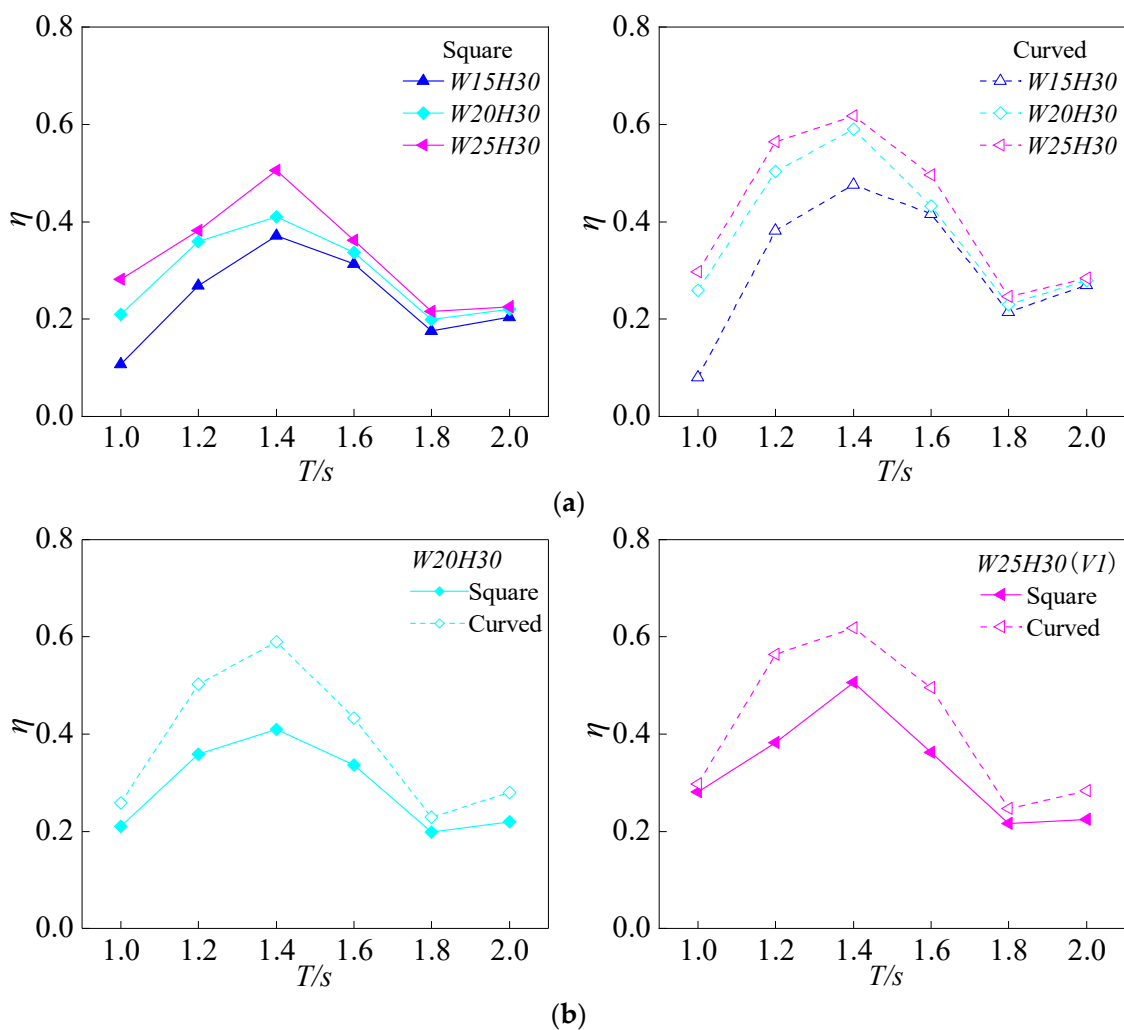


Figure 11. Effects of the opening width on the WECE values of the square and curved WECDs. Period-dependent curves of the WECE of the square and curved WECDs (a) at different opening widths and (b) at the same opening widths.

3.2.4. Effect of the Opening Area

Figure 12 shows the effects of the opening area on the WECE values of the square and curved WECDs. The specific parameters are described in Section 3.1.4. The figure shows that increasing the opening area resulted in an increase in the WECE in the air chamber of the square WECD of 8.7%, 15.7%, 20.6%, and 25.6%, and in the curved WECD, of 12.7%, 24.8%, 30.0% and 38.2%, compared to the WECE values for the minimum opening area. Moreover, the intrachamber wave energy conversion efficiency of the curved WECD was more significantly affected by and more sensitive to the opening area than that of the square WECD. In particular, increasing the opening area significantly enhanced the WECE of the curved WECD over that of the square WECD, especially at an opening area S of 0.060 m^2 . After the opening area exceeded 0.060 m^2 , the superiority of the curved WECD over the square WECD was less prominent.

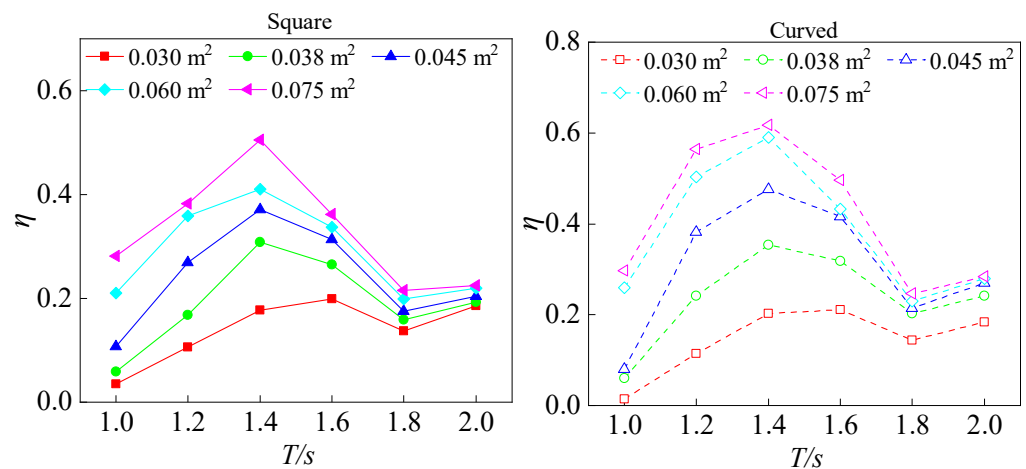


Figure 12. Effects of the opening area on the WECE values of the square and curved WECDs.

3.2.5. Effect of the Chamber Volume

Figure 13 shows the period-dependent curves of the effects of the chamber volume on the WECE values of the square and curved WECDs. The specific parameters are described in Section 3.1.5.

The figure demonstrates that when the chamber volume was reduced to $3/4V_1$, the highest WECE values of the square and curved WECDs were 19.5% and 15.5%, respectively. When the volume of the chamber was reduced to $1/2V_1$, the highest WECE values of the square and curved WECDs were 9% and 5.1%, respectively. Thus, decreasing the chamber volume V reduced the maximum efficiency of wave energy capture in the air chamber of the square and curved WECDs by 31.8% and 35.3%, respectively. This result indicates that when the other factors, such as the opening width and the height of the chamber, were unchanged, the reduction in the chamber volume had a great impact on the WECE. Figure 13b shows that at different chamber volumes, a larger period of the incident wave led to a lower intrachamber WECE value, and that a smaller chamber volume led to the intrachamber WECE of the square WECD being slightly higher than that of the curved WECD.

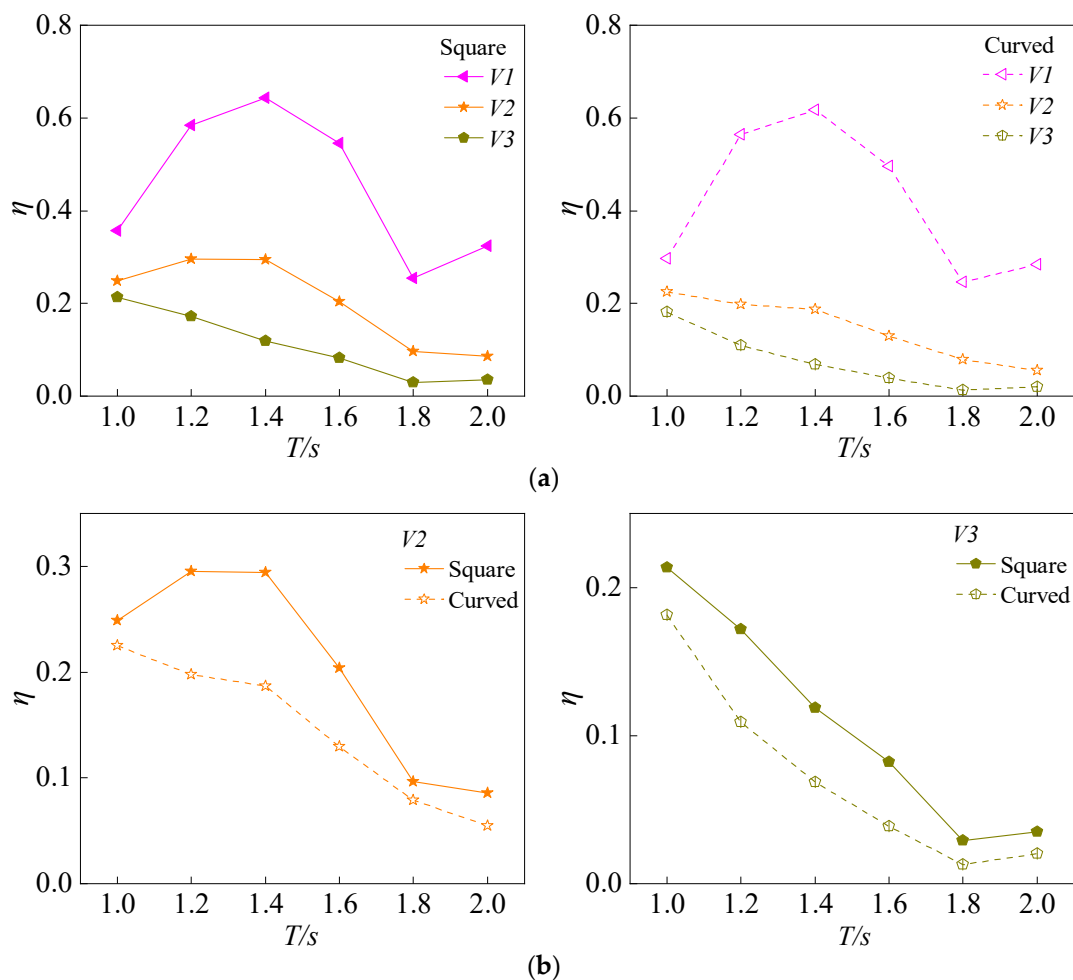


Figure 13. Effects of the chamber volume on the WECE values of the square and curved WECDs. Period-dependent curves of the WECE values of the square and curved WECDs (a) at different chamber volumes and (b) at the same chamber volumes.

4. Conclusions

In this study, model tests were conducted to analyze the operational performance of square and curved wave energy conversion devices (WECDs) under varying incident wave heights, chamber opening lengths and widths, chamber areas, and chamber volumes. The main conclusions reached within the range of the experimental parameters are as follows:

1. The wave surface elevation in the chamber increased and the relative wave height and pressure decreased as the incident wave height increased. Additionally, the WECE increased as the incident wave height decreased. The WECE trend was the same for both the square and curved WECDs, although the WECE values were significantly different.
2. Furthermore, the relative wave height and chamber pressure increased as the opening length, opening width, and opening area of the WECD increased, while the intrachamber WECE increased as the chamber performance increased.
3. Reducing the volume of the air chamber had a different effect on the aerodynamic performance than the other factors, as the relative wave height in the chamber increased and the chamber pressure decreased with decreasing chamber volume, while the intrachamber WECE increased with increasing chamber volume.
4. Both the wave energy conversion and capture efficiency of the curved WECD were better overall than those of the square WECD. It is recommended that in actual projects, a curved WECD should be used.

Author Contributions: Conceptualization, M.Y.; Methodology, H.S.; Investigation, Z.Z.; Resources, X.L.; Writing—original draft, Z.Y.; Writing—review & editing, H.Q. All authors have read and agreed to the published version of the manuscript.

Funding: This work was supported by the NSFC-Shandong Joint Fund (Grant No. U1906231), Natural Science Foundation of Shandong Province (ZR202110280004) and Construction of Marine Environment and Hydraulic Engineering Subjects and Specialty Group (2021XDRHXNXXK01).

Informed Consent Statement: Written informed consent has been obtained from the patient(s) to publish this paper.

Conflicts of Interest: The authors declare no conflict of interest.

References

1. Akpınar, A.; Bingölbali, B.; Van Vledder, G.P. Long-term analysis of wave power potential in the Black Sea, based on 31-year SWAN simulations. *Ocean. Eng.* **2017**, *130*, 482–497. [\[CrossRef\]](#)
2. Akpınar, A.; Kömürçü, M.I. Assessment of wave energy resource of the Black Sea based on 15-year numerical hindcast data. *Appl. Energy* **2012**, *101*, 502–512. [\[CrossRef\]](#)
3. Akpınar, A.; Kömürçü, M.I. Wave energy potential along the south-east coasts of the Black Sea. *Energy* **2012**, *42*, 289–302. [\[CrossRef\]](#)
4. Zheng, C.-W. Global oceanic wave energy resource dataset—With the Maritime Silk Road as a case study. *Renew. Energy* **2021**, *169*, 843–854. [\[CrossRef\]](#)
5. Zheng, C.W.; Li, C.Y. Variation of the wave energy and significant wave height in the China Sea and adjacent waters. *Renew. Sustain. Energy Rev.* **2015**, *43*, 381–387. [\[CrossRef\]](#)
6. Zheng, C.-W.; Pan, J.; Li, J.-X. Assessing the China Sea wind energy and wave energy resources from 1988 to 2009. *Ocean Eng.* **2013**, *65*, 39–48. [\[CrossRef\]](#)
7. Wang, R.Q.; Ning, D.Z.; Mayon, R. Hydrodynamic investigation on the dual-chamber OWC wave energy converter. *Chin. J. Hydrodyn.* **2020**, *35*, 37–41. [\[CrossRef\]](#)
8. He, F.; Li, M.; Huang, Z. An Experimental Study of Pile-Supported OWC-Type Breakwaters: Energy Extraction and Vortex-Induced Energy Loss. *Energies* **2016**, *9*, 540. [\[CrossRef\]](#)
9. Ma, Z.C. An Experimental Study and Performance Evaluation of the Dual Cylindrical Caisson Embodying a U-OWC Wave Energy Converter with Circular Cross Section. Master's Thesis, Dalian University of Technology, Dalian, China, 2020. [\[CrossRef\]](#)
10. Gao, J.; Ma, X.; Zang, J. Numerical investigation of harbor oscillations induced by focused transient wave groups. *Coast. Eng.* **2020**, *158*, 103670. [\[CrossRef\]](#)
11. Gao, J.; Ma, X.; Dong, G.; Chen, H.; Liu, Q.; Zang, J. Investigation on the effects of Bragg reflection on harbor oscillations. *Coast. Eng.* **2021**, *170*, 103977. [\[CrossRef\]](#)
12. Wang, C. The future and development of oscillating water column wave energy conversion device. *Ship Eng.* **2020**, *42*, 14–19. Available online: <https://kns.cnki.net/kcms/detail/detail.aspx?FileName=CANB202008006&DbName=DKFX2020> (accessed on 15 February 2023).
13. Geng, J.; Zhu, R.; Li, M.W.; Zhang, X.L. Study of influencing factors of wave height in the chamber of U-OWC-type wave energy device. *J. Harbin Eng. Univ.* **2020**, *41*, 31–36, 51. [\[CrossRef\]](#)
14. Kim, J.-S.; Kim, K.-H.; Park, J.; Park, S.; Shin, S. A Numerical Study on Hydrodynamic Energy Conversions of OWC-WEC with the Linear Decomposition Method under Irregular Waves. *Energies* **2021**, *14*, 1522. [\[CrossRef\]](#)
15. Ning, D.Z.; Shi, J.; Zou, Q.P. Investigation of hydrodynamic performance of an OWC (oscillating water column) wave energy device using a fully nonlinear HOBEM (higher-order boundary element method). *Energy* **2015**, *83*, 177–188. [\[CrossRef\]](#)
16. Ning, D.Z.; Zhou, Y.; Mayon, R. Experimental investigation on the hydrodynamic performance of a cylindrical dual-chamber Oscillating Water Column device. *Appl. Energy* **2020**, *260*, 114252. [\[CrossRef\]](#)
17. Zhao, X.; Zhang, L.; Li, M. Experimental investigation on the hydrodynamic performance of a multi-chamber OWC-breakwater. *Renew. Sustain. Energy Rev.* **2021**, *150*, 111512. [\[CrossRef\]](#)
18. Doyle, S.; Aggidis, G.A. Development of multi-oscillating water columns as wave energy converters. *Renew. Sustain. Energy Rev.* **2019**, *107*, 75–86. [\[CrossRef\]](#)
19. Du, X.Z.; Zhao, J.Q.; Zhang, Y. Theoretical research on the air pressure in Oscillator Water Column chamber for the wave energy conversion system. *Period. Ocean. Univ. China* **2017**, *47*, 135–141. [\[CrossRef\]](#)
20. Du, X.Z.; Wang, G.Q.; Zhao, Y.; Liu, X.Q. Optimal Design and Comparative Analysis for the Air Chamber Structure of Oscillating Water Column. *Ship Ocean. Eng.* **2018**, *47*, 115–119. Available online: <https://kns.cnki.net/kcms/detail/detail.aspx?FileName=WHZC201805026&DbName=CJFQ2018> (accessed on 15 February 2023).
21. Zhou, J.C. Experimental Study on Hydrodynamic Characteristics of Comb-Type Breakwater-OWC Wave Energy Converter Integrated System. Harbin Engineering University. 2020. Available online: <https://kns.cnki.net/KCMS/detail/detail.aspx?Dbname=CMFD202101&filename=1020156387.nh> (accessed on 1 January 2020).

22. Ning, D.Z.; Wang, R.Q.; Zou, Q.P. An experimental investigation of hydrodynamics of a fixed OWC Wave Energy Converter. *Appl. Energy* **2016**, *168*, 636–648. [[CrossRef](#)]
23. Toyota., K.; Nagata, S. Research for evaluating performance of OWC-type Wave Energy Converter “Backward Bent Duct Buoy”. *Inst. Ocean. Energy Saga Univ.* **2009**, *8*, 901–913. Available online: <https://sc.panda321.com/scholar?Hl=zh-cn&q=Research+for+evaluating+performance+of+OWC-type+Wave+Energy+Converter+%22Backward+Bent+Duct+Buoy> (accessed on 5 January 2023).
24. He, F.; Huang, Z. Characteristics of orifices for modeling nonlinear power take-off in wave-flume tests of oscillating water column devices. *J. Zhejiang Univ. Sci. A* **2017**, *18*, 329–345. [[CrossRef](#)]

Disclaimer/Publisher’s Note: The statements, opinions and data contained in all publications are solely those of the individual author(s) and contributor(s) and not of MDPI and/or the editor(s). MDPI and/or the editor(s) disclaim responsibility for any injury to people or property resulting from any ideas, methods, instructions or products referred to in the content.